Homo- and Copolymerization of 4-Methyl-1-pentene and Ethylene with Group 4 *ansa*-Cyclopentadienylamido Complexes

Guangxue Xu*,† and Danling Cheng

Institute of Polymer Science, Zhongshan University, Guangzhou 510275, P. R. China

Received September 29, 2000; Revised Manuscript Received December 18, 2000

ABSTRACT: A new monocyclopentadienylamido complex, [η^5:η^1-(2,3-Me_2Benz[*e*]Ind)$SiMe_2N^tBu$]$TiCl_2$ (**I**), was synthesized as catalyst precursor. The studies on the homopolymerization and copolymerization of 4-methyl-1-pentene (P) and ethylene (E) were presented, by comparing complex **I** with other CpA complexes and Cp_2M zirconocenes. The complex **I**, activated with methylaluminoxane, provided an enhanced copolymerization activity, an excellent incorporation of 4-methyl-1-pentene into the polyethylene chain, and an increased copolymer molecular weight. Analysis of ^{13}C NMR spectra of polymers, combined with the monomer reactivity ratios and the polymerization results, demonstrated that the regioselectivity of monomer insertion, tacticity, productivity, molecular weights, and polymer microstructure are significantly dependent on the ligand substitution pattern and the metal atom in CpA complexes. The CpA **I**-derived poly(4-methyl-1-pentene-*co*-ethylene)s contained a significant amount of regioirregular arrangement of 4-methyl-1-pentene unit, but with no virtually consecutive 4-methyl-1-pentene sequence. In contrast, the [η^5:η^1-(Me_4C_5)$SiMe_2N^tBu$]$TiCl_2$ (**IV**)-derived copolymers revealed the small clustered sequence (e.g., EPPE) but without any regioirregular arrangement of 4-methyl-1-pentene units. The copolymers prepared with [η^5:η^1-(Flu)$SiMe_2N^tBu$]$TiCl_2$ (**VI**) not only showed quite different microstructure from that based on catalysts **I** and **IV** but also manifested the more pronounced tendency to form an alternating distribution of monomers in the polymer chains. Furthermore, the **VI**-derived copolymer contained neither a regioregular insertion of comonomer nor the consecutive 4-methyl-1-pentene sequences.

Introduction

Constrained geometry catalysts of monocyclopentadienylamido (CpA) titanium complexes are currently of great scientific and technological interest as an important class of metallocene catalysts useful in the copolymerization of ethylene with bulkier α-olefins.[1] These catalysts based on tetramethylcyclopentadienyl and indenyl ligands are especially attractive due to their ability to produce high molecular weight, low-density polyethylenes at high temperatures. Moreover, the well-defined copolymer structure, uniform comonomer distribution, high comonomer incorporation, and high polymer molecular weight and narrow molecular weight distribution in ethylene/α-olefin copolymers are benefits brought about by the CpA catalysts, which dominate the physical or mechanical properties, processabilities, and end applications of olefin copolymers. The ease with which these catalysts incorporate higher olefins appears to be a consequence of the sterically accessible nature of the coordination site. However, further improvement of the copolymerization performance of CpA catalysts by modification of ligand substitution pattern is still the objective of recent studies.[2] Waymouth et al.[2c,3] have observed, by comparing Me_4Cp-based CpA with indenyl-based CpA titaniums, a noticeable influence of the ligand environment in CpA catalysts on the regiospecificity of propylene polymerization and ethylene/norbornene copolymerization. More recently, we have noticed that the benzannelation of 2-methyl-substituted indenyl ligand shows remarkable copolymerization ability in enhancing catalytic activities, comonomer incorporation, and polymer molecular weight for the copolymerization of ethylene with octene[4a,c] or styrene.[4b] We believe that a prerequisite for such rational catalyst design is the knowledge of the influence of different structural patterns on the polymerization performance. Therefore, further studies on CpA catalysts with different ligands contribute to establishing the correlation between the structures of CpA and the polymerization behavior to design a highly efficient CpA catalysts and to understanding the scope and limitation of these types of catalyst systems for the olefin polymerization.

The homo- and copolymerization of 4-methyl-1-pentene and ethylene with CpA catalysts have been attracting our interest. As important polyolefin materials, the 4-methyl-1-pentene/ethylene copolymers have better mechanical properties and processability than the commercial ethylene/1-butene copolymers.[5] Many attempts have been made for decades to synthesize well-defined ethylene/4-methyl-1-pentene copolymers by using traditional heterogeneous Ziegler−Natta catalysts.[5c,6] To the best of our knowledge, the 4-methyl-1-pentene homopolymer and its copolymer are commercially available in Mitsui Petrochem. Co. However, the conventional Ziegler−Natta catalysts were less effective in initiating the copolymerization of ethylene with 4-methyl-1-pentene. The copolymers formed show lower comonomer incorporation and, particularly, a lower polymer molecular weight. Moreover, the copolymers prepared by traditional Ziegler−Natta catalysts are heterogeneous with regard to comonomer incorporation, copolymer composition, and molecular weight distribution. For example, the commercial ethylene/4-methyl-1-pentene copolymer (Mitsui Petrochem. Co.) was separated into three fractions or copolymers containing 11.8, 19.4, and 2.0 mol % of 4-methyl-1-pentene, by the simple extraction of ethyl acetate, ethyl ether, and heptane, respectively.[6] Homogeneous catalysts based on the Cp_2ZrCl_2/MAO system also showed very low catalytic activity, together with low level of monomer incorporation.

† Present address: Catalyst & Polymerization Division, The Technical Department, Formosa Plastics Corp., Point Comfort, Texas 77978. E-mail address: gxxu@ftpc.fpcusa.com.

10.1021/ma001701j CCC: $20.00
Published on Web 02/21/2001

Up to now, a general understanding of their inherent reactivities and their copolymer microstructure is not clear. More importantly, the previous studies still lack the demonstrated evidence of stereospecificity and regioselectivity of monomer insertion in the copolymerization of ethylene and 4-methyl-1-pentene.[7] Given the great interest in the CpA-catalyzed 4-methyl-1-pentene polymers and its copolymers, we carried out a systematic study of the CpA catalysts with different ligands and their catalytic selectivities or regiospecificity for the 4-methyl-1-pentene homopolymerization and its copolymerization. In this paper we reported new constrained geometry catalyst precursors based on modified benz[*e*]indenyl ligand and presented the results of these studies by comparing with other CpA catalysts and Cp_2M catalysts, regarding the effects of the ligand substitution pattern in CpA catalysts on catalytic activity, monomer reactivity ratios, and polymer microstructure.

Experimental Section

General Procedures. All experiments were performed using either the Schlenk techniques or a drybox under a purified nitrogen (N_2) atmosphere. Toluene, diethyl ether, tetrahydrofuran (THF), hexane, and pentane were refluxed over sodium/benzophenone ketyl, from which they were distilled prior to use. Methylene chloride and 4-methyl-1-pentene were purchased from Aldrich, purified by distillation over CaH_2, and stored in a storage flask containing activated 4 Å molecular sieves under high-purity nitrogen. Me_2SiCl_2 was stirred over quinoline overnight, distilled, and stored under N_2 at 5 °C. Polymerization-grade ethylene was purified before its use, by passing it through columns containing a supported oxygen-removal MnO and an activated 4 Å molecular sieve. Methylaluminoxane (MAO) was prepared as described in the literature.[8] Its TMA content, determined by NMR, was about *26* mol %. 2,3-Dimethylbenz[*e*]indene (**1**) was synthesized as described in the literature[9] and characterized by elemental analysis and the NMR spectrum. [η^5:η^1-(2-MeBenz[*e*]Ind)$SiMe_2N^tBu$]$TiCl_2$ (**II**),[4] [η^5:η^1-(Benz[*e*]Ind)$SiMe_2(N^tBu)$]$TiCl_2$ (**III**),[4] [η^5:η^1-(Me_4C_5)$SiMe_2N^tBu$]$TiCl_2$ (**IV**),[1b,c,2c] [η^5:η^1-(Ind)$SiMe_2N^tBu$]$TiCl_2$ (**V**),[10] [η^5:η^1-(Flu)$SiMe_2N^tBu$]$TiCl_2$ (**VI**),[11] [η^5:η^1-(C_5H_4)$SiMe_2N^tBu$]$TiCl_2$ (**VII**),[2c,12] *rac*-$Me_2Si(Ind)_2ZrCl_2$ (**IX**),[13] *rac*-Me_2Si(2-MeInd)$_2ZrCl_2$ (**X**),[14] *rac*-Me_2Si(Benz[*e*]-Ind)$_2ZrCl_2$ (**XI**),[15] and *rac*-Me_2Si(2-MeBenz[*e*]Ind)$_2ZrCl_2$ (**XII**)[15] compounds were prepared as described in the literature. *rac*-Et(Ind)$_2ZrCl_2$ (**VIII**) and other reagents were purchased from Aldrich and used without further purification. The ^{1}H NMR spectra were performed on an AM-250 Bruker spectrometer, and the elemental analyses were carried out on a PE-2400 analyzer.

Synthesis of {η^1:η^5-[(*tert*-Butylamido)dimethylsilyl]-(2,3-dimethylbenz[*e*]indenyl)}titanium Dichloride (I). (*tert*-Butylamino)dimethyl(2,3-dimethylbenz[*e*]indenyl)-silane (2). To a stirred suspension of 2,3-dimethylbenz[*e*]-indene (**1**) (19.42 g, 100 mmol) in 50 mL of diethyl ether at 0 °C was added dropwise a 2.5 M solution of butyllithium in hexane (40 mL, 100 mmol). After stirring for 1 h at 0 °C and for 4 h at room temperature, the resulting solution was quickly transferred to an addition funnel under a nitrogen atmosphere and then added dropwise at 0 °C to a solution of dichlorodimethylsilane (250 mL, 2.06 mol) in diethyl ether (100 mL). The mixture was stirred while warming to 25 °C over a period of 5 h, and then the solvent and the excess dichlorodimethylsilane were removed under vacuum. After precipitating lithium chloride with methylene chloride, followed by the filtration and solvent removal, a slightly yellow solid was obtained (21.51 g, 75% yield). ^{1}H NMR ($CDCl_3$ at 25 °C): δ 7.34−8.40 (m, 6H, arom H), 3.53 (s, 1H, H−C_5(1)), 2.55 (s, CH_3), 2.25 (s, CH_3), 0.60 (s, 6H, $SiCH_3$). Anal. Calcd for $C_{17}H_{19}SiCl$: C, 71.18; H, 6.68. Found: C, 71.07; H, 6.71.

To a solution of this crude chlorodimethyl(2,3-dimethylbenz-[*e*]indenyl)silane (21.51 g, 75 mmol) in diethyl ether (100 mL) at 0 °C was added a solution of lithium *tert*-butylamide (5.93 g, 75 mmol) in diethyl ether (25 mL) over a period of 1 h. Stirring overnight at room temperature produced a light yellow suspension. After the removal of volatiles under vacuum, the lithium chloride was precipitated with methylene chloride. A fine white precipitate of LiCl was then separated by filtration. Evaporation of the filtrate and extraction of the residue from 150 mL of pentane at room temperature, followed by the removal of solvent under vacuum of 15 mTorr, afforded 17.11 g (70.5% yield) of **2** as a colorless viscous oil. ^{1}H NMR ($CDCl_3$ at 25 °C): δ 7.35−8.56 (m, 6H, arom H), 3.60 (s, 1H, H−C_5-(1)), 2.58 (s, 3H, CH_3), 2.33 (s, 3H, CH_3), 1.28 (s, 9H, $NCCH_3$), 0.75 (s, br, 1H, NH), 0.04 (s, 3H, $SiCH_3$), −0.20 (s, 3H, $SiCH_3$). Anal. Calcd for $C_{21}H_{29}NSi$: C, 77.96; H, 9.04; N, 4.33. Found: C, 78.05; H, 8.97; N, 4.38.

{*tert*-Butyl[dimethyl(2,3-dimethylbenz[*e*]indenyl)silyl]amido}dilithium (3). A solution of 17.11 g (59.64 mmol) of (*tert*-butylamino)dimethyl(2,3-dimethylbenz[*e*]indenyl)silane (**2**) in 100 mL of diethyl ether was cooled to −78 °C. To this solution, a solution of 2.5 M *n*-butyllithium (119.3 mmol) in hexane (47.8 mL) was added over a period of 40 min. After the solution was stirred for 2 h at −78 °C, it was gradually warmed to room temperature and stirred overnight, after which an yellow precipitate was collected by filtration. The product residue was washed with toluene and pentane and then dried under vacuum (10^{-6} Torr) to obtain 19.80 g (99.0% yield) of **3** as an yellow powder. Anal. Calcd for $C_{21}H_{27}NSiLi_2$: C, 75.20; H, 8.11; N, 4.18. Found: C, 75.15; H, 8.17; N, 4.08.

{η^1:η^5-[(*tert*-Butylamido)dimethylsilyl](2,3-dimethylbenz[*e*]indenyl)}titanium Dichloride (I). To a suspension of {*tert*-butyl[dimethyl(2,3-dimethylbenz[*e*]indenyl)-silyl]amido}dilithium (**3**) (19.80 g, 59.0 mmol) in 100 mL of toluene at −78 °C was added a solution of $TiCl_4(THF)_2$ (19.23 g, 59.0 mmol) in toluene (50 mL) over a period of 1 h. After slowly warming the mixture to room temperature, the red suspension was stirred 48 h and then filtered. The vacuum removal of toluene from the supernatant led to a sticky dark red solid. A red/orange microcrystalline solid of [η^5:η^1-(2,3-Me_2-Benz[*e*]Ind)$SiMe_2N^tBu$]$TiCl_2$ (**I**) (4.68 g, 18% yield) was collected by sublimation under 120 °C and 10^{-4} Torr. ^{1}H NMR ($CDCl_3$ at 25 °C): δ 8.43 (m, 1H, arom H), 7.45−8.60 (m, 5H, arom H), 2.88 (s, 3H, CH_3), 2.53 (s, 3H, CH_3), 1.30 (s, 9H, $NCCH_3$), 0.93 (s, 3H, $SiCH_3$), 0.66 (s, 3H, $SiCH_3$). ^{13}C NMR ($CDCl_3$): δ136.3, 135.4, 132.6, 131.2, 129.7, 129.5, 129.2, 128.8, 127.6, 126.7, 119.5, 98.8, 63.1, 32.5, 25.6, 3.4, 0.9. Anal. Calcd for $C_{21}H_{27}Cl_2NSiTi$: C, 57.28; H, 6.18; N, 3.18. Found: C, 57.26; H, 6.13; N, 3.21.

4-Methyl-1-pentene Homopolymerizations. A 250 mL reactor equipped with a magnetic stirrer was attached to a high-vacuum line and then sealed under a nitrogen atmosphere. Freshly distilled toluene (50 mL) was introduced through a syringe, followed by adding 4-methyl-1-pentene (50 mL, 3.96 mol/L) and methylaluminoxane (MAO) (20.0 mmol). The bottle was placed in a bath at 45 °C and stirred for 10 min. The solution of metallocene catalyst (10 μmol in 3 mL of toluene) was then added to start the polymerization. The polymerization was carried out for 30 min and then quenched with acidic methanol (150 mL). The precipitated polymer was filtered, washed with methanol, and then dried overnight in a vacuum oven at 60 °C.

Representative 4-Methyl-1-Pentene/Ethylene Copolymerization. The copolymerization of 4-methyl-1-pentene with ethylene was carried out in a 500 mL high-pressure reactor equipped with a mechanical stirrer. Toluene (65 mL) and 4-methyl-1-pentene (20 mL, 1.59 M) were added to the reactor with a syringe under a nitrogen atmosphere, followed by the addition of MAO solution (5.0 mmol in 10 mL of toluene). The reactor was placed in a bath and equilibrated at 45 °C. The inert gas was removed, and then ethylene was introduced into the reactor. After the thermal equilibration at 45 °C for 10 min, ethylene (2.2 bar pressure) was continually supplied through a mass-flow meter until the reaction mixture was saturated with ethylene. The polymerization was started by adding a solution of metallocene catalyst (5 μmol in 5 mL of toluene) with a syringe. The mixture was maintained under

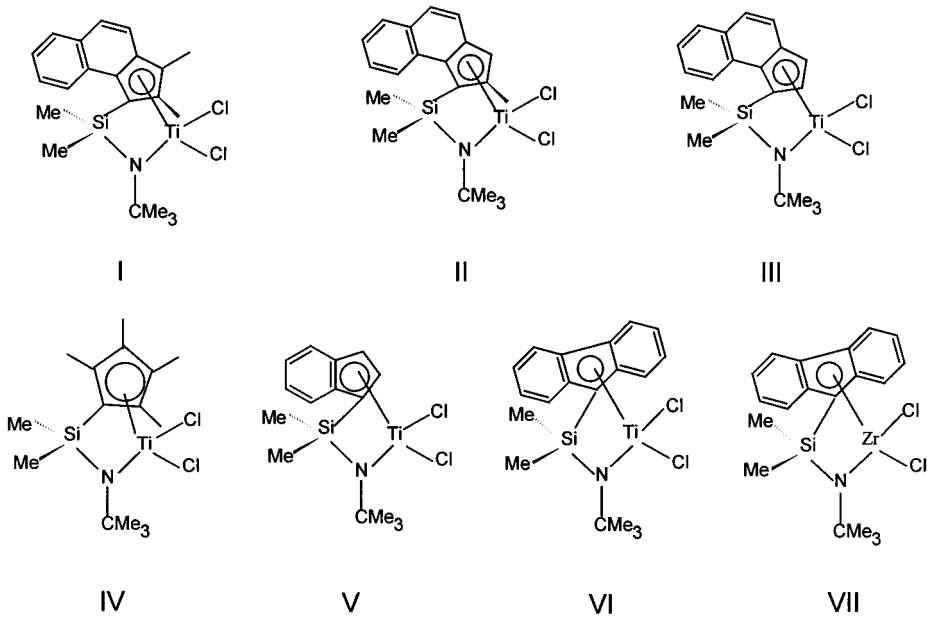

Figure 1. CpA catalysts for homo- and copolymerization of 4-methyl-1-pentene and ethylene.

a constant ethylene pressure of 2.2 bar during the polymerization. Ethylene concentrations were determined by using both Henry−Gesetz expression[16] and solubility measurement by GC. Polymerization was conducted for 30 min and then quenched with methanol (100 mL). Polymers were precipitated by pouring the reaction mixture into acidic MeOH (350 mL) and stirring overnight. The precipitated polymer was washed with methanol, subsequently collected by filtration, and dried in a vacuum oven at 60 °C.

Polymer Analyses. The ^{13}C NMR spectra of the copolymers were recorded at 110 °C using an AM-250 Bruker spectrometer with a 30° pulse angle, 2 s delay, and at least 48 000 data scans. The samples were prepared by dissolving 50 mg of polymer in 0.4 mL of 1,1,2,2-tetrachloroethane-d_2. The 4-methyl-1-pentene content in the copolymer was estimated from the ^{13}C NMR spectra.[6] The molecular weight (M_w) and molecular weight distribution (M_w/M_n) of the copolymer were determined by gel permeation chromatography at 135 °C using a Water 150-C ALC GPC instrument equipped with Waters μStyragel columns (exclusion limits for polystyrene 10^3, 10^4, and 10^6 Å) using 1,2,4-trichlorobenzene as solvent and polystyrene as standards. The melting temperature, crystallinity, and glass transition temperature were determined by differential scanning calorimetry (DSC) with a Perkin-Elmer DSC-7 system at a heating rate of 10 °C/min. Any thermal history effect in the polymers was eliminated by first heating the specimen to 180 °C, cooling at 10 °C/min to −100 °C, and then recording the second DSC scan. The percent crystallinity was calculated from the heat of fusion using the expression $X_c = \Delta H_f / \Delta H_f^0$, where ΔH_f is the heat of fusion of the sample as determined from the DSC curve and ΔH_f^0 is the heat of fusion of folded-chain polyolefin crystals (293 J/g for polyethylene).[17]

Results and Discussion

Catalyst Synthesis. Shown in Figure 1 are seven CpA catalysts we used to probe the influence of the ligand substitution pattern in catalysts on the catalytic activity, 4-methyl-1-pentene incorporation, and copolymer microstructure. The new constrained geometry complex **I**, [η^5:η^1-(2,3-Me_2BenzInd)SiMe_2N^{t}Bu]TiCl_2, was prepared with a yield of 18%, by reacting {*tert*-butyl-[dimethyl(2,3-dimethylbenz[*e*]indenyl)silyl]amido}-dilithium (**3**) with TiCl_4(THF)$_2$ in toluene, as described in detail in the Experimental Section. It was found that a higher dilution and moderate mixing of toluene solution of TiCl_4(THF)$_2$ and [(2,3-Me_2BenzInd)SiMe_2N^t-Bu]Li_2 could slightly increase the yield. A higher yield of the complex **I** could be achieved via amine elimination route.[18] The reaction of neutral Cp−amide ligand (**2**) with Ti$(NMe_2)_4$ in refluxing toluene over 3 days led to complete production of the ligated bis(dimethylamido)-titanium complex. The bis(dimethylamide) can be converted to the dichloride (**I**) (yield, 58.5% based on Ti$(NMe_2)_4$) by treatment with excess Me_3SiCl in methylene chloride. The complexes **II**−**XII** were synthesized according to the literature procedures described in Experimental Section.

4-Methyl-1-Pentene Homopolymerization. Homopolymerizations of 4-methyl-1-pentene were carried out in toluene solution with CpA complexes (**I**−**VII**) or, for comparison, with the Cp_2M zirconocenes (**VIII**−**XII**). Table 1 lists the results of these experiments. Of the all catalysts examined, the Cp_2M zirconocenes exhibit the highest productivity, followed by CpA titaniums (**I**−**VI**) and then CpA zirconium **VII**. As compared with Cp_2M zirconium systems, the open and accessible coordination nature of CpA catalysts does not contribute to enhancing reaction activity for the 4-methyl-1-pentene polymerization but does result in lower stereospecificity and regiospecificity in 4-methyl-1-pentene polymerization. However, we found that higher reaction temperature obviously enhanced the catalyst activity of the CpA titanium complex. For example, the polymerization productivity or catalyst activity of the catalysts **I** and **II** is increased by a factor of 2 when the reaction temperature is increased to 85 °C.

One can notice the significant influence of the ligand substitution pattern in CpA complex on the polymerization. As revealed in Table 1, the catalysts **I** and **II** exhibit more than 2 times higher activity than other CpA systems, together with high polymer molecular weight. This is probably the effect of the increased electron-donating character of the methyl-substituted benz[*e*]indenyl ligand, which may result in a decrease in chain termination (i.e., β-H elimination) and/or increased the stabilization of the active species toward reduction. On the other hand, the bulkier substituted benz[*e*]indenyl substituent of catalysts **I** and **II** makes the titanium center sterically rather inaccessible, pos-

Table 1. 4-Methyl-1-pentene Homopolymerizations with CpA Catalysts and Zirconocenes[a]

run	catalyst	productivity[b]	$10^{-3}M_w$[c]	M_w/M_n[c]	mmmm (%)[d]	2,1-units (%)[d]
1	[Me_2Si(2,3-Me_2−Benz[*e*]Ind)(N^tBu)]$TiCl_2$ (**I**)	2760	218	2.32	38.5	0.8
2	[Me_2Si(2,3-Me_2−Benz[*e*]Ind)(N^tBu)]$TiCl_2$ (**I**)[e]	5600	189	2.01	37.9	0.9
3	[Me_2Si(2-Me−Benz[*e*]Ind)(N^tBu)]$TiCl_2$ (**II**)	2510	164	2.07	32.8	1.6
4	[Me_2Si(2-Me−Benz[*e*]Ind)(N^tBu)]$TiCl_2$ (**II**)[e]	5050	157	2.00	33.0	1.5
5	[Me_2Si(Benz[*e*]Ind)(N^tBu)]$TiCl_2$ (**III**)	1420	98	1.95	24.5	2.5
6	[Me_2Si(Me_4Cp)(N^tBu)]$TiCl_2$ (**IV**)	1250	145	2.01	5.5	3.4
7	[Me_2Si(Ind)(N^tBu)]$TiCl_2$ (**V**)	750	78	2.25	17.4	4.5
8	[Me_2Si(Flu)(N^tBu)]$TiCl_2$ (**VI**)	295	457	2.45	30.5	0
9	[Me_2Si(Flu)(N^tBu)]$ZrCl_2$ (**VII**)	170	460	2.51	12.3	0
10	*rac*-Et$(Ind)_2ZrCl_2$ (**VIII**)	4100	75	2.05	85.6	1.5
11	*rac*-$Me_2Si(Ind)_2ZrCl_2$ (**IX**)	4200	85	1.98	88.5	1.2
12	*rac*-Me_2Si(2-Me−$Ind)_2ZrCl_2$ (**X**)	3250	135	2.08	90.0	0.8
13	*rac*-Me_2Si(Benz[*e*]$Ind)_2ZrCl_2$ (**XI**)	7600	95	1.95	92.5	0.8
14	*rac*-Me_2Si(2-Me−Benz[*e*]$Ind)_2ZrCl_2$ (**XII**)	5200	168	2.10	94.1	0.4

[a] Polymerization conditions: [4-methyl-1-pentene] = 3.96 mol/L, [cat] = 100 μmol/L, MAO/M = 2000 (M = Zr, Ti), solvent = toluene (total solvent = 100 mL), polymerization time (t_p) = 30 min, polymerization temperature (T_P) = 45 °C. [b] Productivity in kg of polymer/[(mol of metal) (mol of monomer) h]. [c] Determined by gel permeation chromatography. [d] Determined by ^{13}C NMR spectrum. [e] Polymerization temperature (T_p) = 85 °C.

Table 2. Ethylene/4-Methyl-1-pentene Copolymerization Using Catalysts I−XII[a]

run	catalyst [b]	[E] (M)	[MP] (M)	yield (g)	productivity[c]	incorp[d] (mol %)	T_g[e] (°C)	$10^{-3}M_w$[f]	M_w/M_n
1	**I**	0.21	1.59	12.3	27 333	45.7	−22.5	379	1.96
2	**II**	0.21	1.58	9.5	21 229	43.5	−28.5	337	1.98
3	**III**	0.22	1.57	6.3	14 078	36.9	−36.2	215	2.02
4	**IV**	0.21	1.58	6.5	14 525	40.7	−31.8	298	2.10
5	**V**	0.20	1.56	4.5	10 227	32.5	−40.2	124	2.03
6a	**VI**	0.23	1.57	2.0	4 445	44.5	−25.6		
6b	**VI**	0.23	0.95	2.1	7 122	40.6	−31.2	480	2.21
7	**VII**	0.21	1.58	0.6	1 341	28.8	−47.0	450	2.15
8	**VIII**	0.20	1.55	4.3	9 829	26.5	−48.5	98	2.30
9	**IX**	0.24	1.59	4.5	9 836	28.2	−46.9	119	2.35
10	**X**	0.22	1.57	3.6	8 045	28.4	−45.3	158	2.21
11	**XI**	0.20	1.59	4.5	10 056	30.5	−39.8	123	2.01
12	**XII**	0.21	1.58	5.0	11 173	31.9	−38.9	195	1.98

[a] Conditions: ethylene pressure = 2.0−2.5 bar, [cat] = 50 μmol/L, MAO/M = 1000 (M = Zr, Ti), solvent = toluene (total solvent = 100 mL), t_p = 30 min, T_p = 45 °C. [b] **I** = [Me_2Si(2,3-Me_2−Benz[*e*]Ind)(N^tBu)]$TiCl_2$, **II** = [Me_2Si(2-Me-Benz[*e*]-Ind)(N^tBu)]$TiCl_2$, **III** = [Me_2Si(Benz[*e*]Ind)(N^tBu)]$TiCl_2$, **IV** = [Me_2Si(Me_4Cp)(N^tBu)]$TiCl_2$, **V** = [Me_2Si(Ind)(N^tBu)]$TiCl_2$, **VI** = [Me_2Si(Flu)(N^tBu)]$TiCl_2$, **VII** = [Me_2Si(Flu)(N^tBu)]$ZrCl_2$, **VIII** = *rac*-Et$(Ind)_2ZrCl_2$, **IX** = *rac*-$Me_2Si(Ind)_2ZrCl_2$, **X** = *rac*-Me_2Si(2-Me-Ind)$_2ZrCl_2$, **XI** = *rac*-Me_2Si(Benz[*e*]$Ind)_2ZrCl_2$, **XII** = *rac*-Me_2Si(2-Me-Benz[*e*]$Ind)_2ZrCl_2$. [c] Productivity in kg of P(E-*co*-MP)/[(mol of metal) (mol of total monomers) h]. [d] 4-Methyl-1-pentene incorporation determined by NMR. [e] Determined by DSC. [f] Determined by GPC.

sibly thus suppressing detrimental β-agostic interactions which promotes the olefin insertions relative to chain termination by β-H transfer or sterically stabilizes the active species.

At the same time, the findings in Table 1 also show a noticeable influence of the ligand environment on the stereospecificity and the regiospecificity of CpA catalysts. CpA titanium catalysts based on tetramethylcyclopentadienyl and indenyl rings lead to lower stereospecificity and much higher regioirregularities in the poly(4-methyl-1-pentene) chain. In contrast, the benz[*e*]indenyl-based CpA catalysts show, as expected, a remarkable increase in propagation stereoregularity [mmmm] and a significant decrease in monomer insertion regiospecificity (i.e., 2,1-insertion) for 4-methyl-1-pentene polymerization. Quantitative ^{13}C NMR analysis reveals that, for instance, the more sterically hindered benz[*e*]ind-based catalysts (**I** and **II**) produce polymers with about 36.0−82.2% less 2,1-insertion than other CpA catalysts examined. The bulkier benzoannelated substituents in catalysts **I** and **II** presumably force the growing chain and monomer insertion into a more constrained conformation, which in turn favors a higher steric control.

It is notable that the fluorenyltitanium CpA catalyst (**VI**) and fluorenylzirconium CpA catalyst (**VII**) yield highly regioregular polymer but with different stereoregularity [mmmm]. It seems that, for CpA catalysts, the higher regiospecificity is strongly associated with ligand pattern and the nature of monomer,[4b,11] while higher stereospecificity is related to the natures of both metal atom and ligand substitution pattern. The catalysts with a fluorenyl ligand produce the largest molecular weight, because both steric and electronic effects possibly suppress the chain transfer and chain termination reactions.[19]

Copolymerizations of 4-Methyl-1-pentene and Ethylene. To compare the catalytic performance of CpA catalysts and Cp_2M complexes and to evaluate the influence of the ligand substitution pattern in CpA catalysts on the copolymerization performance, we conducted the 4-methyl-1-pentene/ethylene copolymerization by using MAO-activated metallocenes **I**−**XII** at similar polymerization conditions (Table 2). It can clearly be observed that, in contrast with the 4-methyl-1-pentene homopolymerization, CpA catalysts provide a higher catalytic activity and polymer molecular weight, and better comonomer incorporation than the Cp_2M complexes with identical ligand substitution pattern, for the 4-methyl-1-pentene/ethylene copolymerization. Attempts to compare metal effects were carried out by using fluorenyltitanium (**VI**) and fluorenylzirconium (**VII**). The results for **VI** and **VII** indicate that the nature of the metal atoms (Ti and Zr) does have a noticeable influence on the catalytic activity and the 4-methyl-1-pentene incorporation. The catalyst **VI** shows higher productivity (more than 3 times) and higher 4-methyl-1-pentene incorporation than the complex **VII**, indicating that CpA titanium complex is more active than CpA zirconium catalyst for the 4-methyl-1-pentene/ethylene copolymerization.

Table 3. 4-Methyl-1-pentene Copolymerization with Ethylene by Using [η^5:η^1-(2,3-Me_2Benz[*e*]Ind)−$SiMe_2N^tBu$]$TiCl_2$ (I)/MAO Catalyst[a]

run	T_p (°C)	[E] (M)	[MP] (M)	productivity,[b]	incorp[c] (mol %)	T_g[d] (°C)	T_m[d] (°C)	cryst[d] (%)	$10^{-3}M_w$[e] (g/mol)	M_w/M_n[e]
13	0	0.21	0.95	924	6.5	−65.9	96	27	640	1.95
14	15	0.22	0.95	7 241	10.8	−60.1	65	12	495	1.98
15	25	0.22	0.95	9 463	15.1	−56.7	n.d.[f]	nil		
16	35	0.21	0.95	12 650	20.0	−51.0	n.d.[f]	nil	392	2.01
17	45	0.21	0.95	28 414	37.8	−38.2	n.d.[f]	nil	365	2.15
18	85	0.21	0.95	29 500	40.5	−31.8	n.d.[f]	nil	368	2.10
19	45	0.32	1.09	30 681	35.4	−40.1	n.d.[f]	nil	376	2.18
20	45	0.54	1.09	34 221	28.2	−46.5	n.d.[f]	nil	341	2.22
21	45	0.10	1.09	20 790	42.1	−27.5	n.d.[f]	nil	373	2.21
22	45	0.11	0.54	21 875	38.6	−38.6	n.d.[f]	nil	345	2.30
23	45	0.23	0	57 143	0	−75.0	132	60	546	2.10
24	45	0.21	0.08	41 379	8.5	−62.5	85	21	325	2.19
25	45	0.21	0.16	34 595	12.5	−55.2	57	10	389	2.03
26	45	0.21	0.40	32 787	25.2	−47.5	n.d.[f]	nil	375	2.24
27	45	0.22	0.79	29 703	35.5	−37.8	n.d.[f]	nil	365	2.18
28	45	0.21	1.65	27 204	44.6	−25.7	n.d.[f]	nil	358	2.05
29	45	0.21	3.96	16 592	46.4	−20.4	n.d.[f]	nil	384	2.30
30	45	0	1.58	2 932	100	28.7	165	nil	219	2.12

[a] Polymerization conditions: ethylene pressure = 1.0−5.5 bar depending on each experiment condition, [cat] = 50 μmol/L, MAO/M = 1000 (M = Zr, Ti), solvent = toluene (total solvent = 100 mL), t_p = 30 min. [b] Productivity in kg of P(E-*co*-MP)/[(mol of metal) (mol of total monomers) h]. [c] 4-Methyl-1-pentene incorporation in copolymer, determined by NMR. [d] Determined by DSC. [e] Determined by GPC. [f] Not detectable.

On the other hand, Table 2 reveals the influence of the ligand substitution pattern in CpA catalysts examined on the 4-methyl-1-pentene/ethylene copolymerization. Summing up the results of the productivity or copolymerization activity, the following ranking can be stated: [Me_2Si(2,3-Me_2Benz[*e*]Ind)(N^tBu)]$TiCl_2$ (**I**) > [Me_2Si(2-Me-Benz[*e*]Ind)(N^tBu)]$TiCl_2$ (**II**) > [Me_2Si(Me_4-Cp)(N^tBu)]$TiCl_2$ (**IV**) ≥ [Me_2Si(Benz[*e*]Ind)(N^tBu)]$TiCl_2$ (**III**) > [Me_2Si(Ind)(N^tBu)]$TiCl_2$ (**V**) > [Me_2Si(Flu)-(N^tBu)]$TiCl_2$ (**VI**) > [Me_2Si(Flu)(N^tBu)]$ZrCl_2$ (**VII**). The 4-methyl-1-pentene incorporation and polymer molecular weight also follow similar order, with the exception of the fluorenyl-based CpA catalysts (**VI**−**VII**). The electronic effect and steric advantage of the ligand substitution in CpA catalysts that discussed in 4-methyl-1-pentene homopolymerizations hold true for the 4-methyl-1-pentene/ethylene copolymerization. These findings suggest that the high electronic density and preferred steric advantages of the Cp-ring stabilize the active species against deactivation and chain transfer or termination, increase the rate of monomer insertion to the metal−alkyl bond, and enhance the number of active sites,[1,2,4c,20] thus increasing overall catalytic activity, polymer molecular weight, and even the chain propagation rate. The electron-withdrawing or the less electron-donating substituents (such as indenyl and fluorenyl) provide lower activity. Similar to 4-methyl-1-pentene homopolymerization system, the fluorenyl-substituted complex **VI** and **VII** produce copolymers with highest molecular weights.

The complex **I** is so far the most productive CpA catalysts; analogous copolymerizations with [Me_2Si(Me_4-Cp)(N^tBu)]$TiCl_2$ (**IV**) and [Me_2Si(Ind)(N^tBu)]$TiCl_2$ (**V**) are approximately 2−3 times less productive (Table 2). Table 3 summarizes the results regarding the 4-methyl-1-pentene/ethylene copolymerization with catalyst **I** for various copolymerization conditions. The activity of CpA catalyst **I** increases with increasing polymerization temperature from 0.92×10^6 at 0 °C to 29.5×10^6 g of polymer/[(mol of Ti) (mol of monomers) h] at 85 °C. We observed that, even at temperatures as high as 120 °C, the complex **I** lead to a high polymer molecular weight ($M_w = 31.5 \times 10^4$ g/mol) with a narrow the molecular weight distribution ($M_w/M_n = 2.18$). It is interesting that, at high polymerization temperatures of 120 °C, the complex **I** show no decrease in its activity (28.2×10^6 g of polymer/[(mol of Ti) (mol of monomers) h]. These findings indicate that the catalyst **I** is remarkable stable and that in this case the CpA titanium **I** is less easily deactivated or reduced into multicenter active species.[8,9]

The molecular weight (M_w) of the coploymers prepared with **I**/MAO catalyst shows strong temperature dependence, increasing linearly as the polymerization temperature (T_p) decreases. This can be attributed to change in the ratio of chain propagation (k_p) to chain transfer (k_{tr}) (e.g., β-H elimination) as the polymerization temperature is changed. The chain transfer or termination via β-H elimination requires a high activation energy;[8] the lowering of the T_p decreases the rate of β-hydride elimination and thus increases the M_w of the copolymers. 4-Methyl-1-pentene incorporation in the copolymer, however, increases with the increase of reaction temperature. The fact that higher temperature favors higher 4-methyl-1-pentene incorporation may be attributed to higher activation energies (ΔE) for the migratory insertion and propagation of 4-methyl-1-pentene than ethylene.

As revealed by runs 19−30 of Table 3, the catalytic activity of **I** decreases with increasing 4-methyl-1-pentene concentration or decreasing ethylene concentration. This occurs because the insertion of ethylene is faster than that of 4-methyl-1-pentene, possibly because of a steric hindrance at the active site for the latter molecule. The 4-methyl-1-pentene incorporation is, however, proportional to its content in the feed. The molecular weight of the copolymer produced with **I**/MAO is essentially independent of monomer concentration, which is consistent with termination occurring due to β-H transfer to a coordinated monomer [15,21] or due to alkene C−H activation.[22] We observed that, with increasing the comonomer content, the polymer molecular weight decreased for the styrene/ethylene copolymerization but slightly increased for the ethylene/octene copolymerization with the CpA catalyst **I**. Obviously, the extent of transfer reaction is dependent on the nature of the comonomer, which is inserted before an ethylene molecule. For a more detail description of this phenomenon, additional experiments including those with other CpA catalysts have still to be performed.

The incorporation of 4-methyl-1-pentene is associated with a change in the glass-transition temperature (T_g) and the melting temperature (T_m) of the ethylene/4-

Table 4. Copolymerization of 4-Methyl-1-pentene and Ethylene with [η^5:η^1-(2,3-Me_2Benz[*e*]Ind)−$SiMe_2N^tBu$]$TiCl_2$ (I)/MAO Catalyst[a]

run	[E] (M)	[MP] (M)	incorp (mol %)[b]	x[c]	y[d]	ξ[e]	η
31	0.11	2.19	46.3	0.050	1.16	0.045	0.136
21	0.10	1.09	42.1	0.092	1.38	0.114	0.481
22	0.11	0.54	38.6	0.185	1.59	0.332	1.031
32	0.21	1.65	41.6	0.127	1.40	0.209	0.643
33	0.21	1.09	40.2	0.193	1.63	0.372	1.083
34	0.32	2.19	40.2	0.146	1.48	0.251	0.799
19	0.32	1.09	35.4	0.294	1.83	0.501	1.435
35	0.54	1.09	25.2	0.495	2.97	0.682	1.685
36	0.54	0.54	22.1	1.000	3.53	0.860	1.960

[a] Polymerization conditions: ethylene pressure = 1.0−5.5 bar depending on each experiment condition, [cat] = 50 μmol/L, MAO/M = 1000 (M = Zr, Ti), solvent = toluene (total solvent = 100 mL). [b] 4-Methyl-1-pentene incorporation in copolymer, determined by NMR. [c] $x = [M_1]/[M_2]$, x is the molar ratio of comomoners. [d] y = E/MP in copolymer.

methyl-1-pentene copolymer. The T_g of the copolymers increased with increasing comonomer incorporation, while T_m and the crystallinity of the copolymers significantly decreased with increasing comonomer incorporation. The melting temperature (T_m) and crystallinity can be attributed to a blocky microstructure, which contains sufficiently long sequences of monomer units in the polymer backbone to generate crystalline domains. One can notice that a 6.5 mol % of 4-methyl-1-pentene incorporation decreases the melting temperature (T_m) from 132 to 96 °C and the copolymer crystallinity from 60 to 27%. When the comonomer incorporation is increased to 15 mol %, the DSC curve has only a sharp T_g, without any detectable melting point and crystallinity. This indicates that the copolymers with more than 15 mol % of comonomer incorporation do not possess sufficiently long comonomer sequences to form small crystalline domains. This result is coincident with these of the coplymerization kinetics and ^{13}C NMR analysis (vide infra).

Determination of 4-Methyl-1-pentene/Ethylene Reactivity Ratios. To calculate the 4-methyl-1-pentene/ethylene reactivity ratios for the CpA and Cp_2M catalysts examined in this study according to Kelen and Tüdös methodology,[23,24] several copolymerizations of 4-methyl-1-pentene and ethylene were carried out with MAO-activated **I**−**XII** over a broad range of monomer ratios at 45 °C. Data for CpA **I**-catalyzed copolymerization and its Kelen−Tüdös plot are shown in Table 4 and Figure 2 as a typical example. Table 5 lists the results of the reactivity ratio calculations for metallocenes for the 4-methyl-1-pentene/ethylene copolymerization. Compared with the Cp_2M catalysts, the CpA catalysts give much lower r_1 values, indicating a reduced preference for insertion of ethylene over 4-methyl-1-pentene into a M−E* active center. On the other hand, for the CpA ethylene/4-methyl-1-pentene system, the r_1 and r_2 values differ much more from catalyst to catalyst, reflecting the ligand substitution influence of CpA catalysts. Of all the CpA catalysts, **I**, **II**, **III**, and **VI** show the lowest r_1 and r_2 values. The lower r_1, the stronger is the tendency to insert 4-methyl-1-pentene over ethylene into M−E* active center and to produce a copolymer with an alternating structure. The lowest r_2 values for catalysts **I**, **II**, **III**, and **VI** clearly illustrate that these CpA catalysts strongly discourage 4-methyl-1-pentene homopolymerization, because of the highly steric influence between the ligand substitution and the last inserted 4-methyl-1-pentene unit, as evidenced with

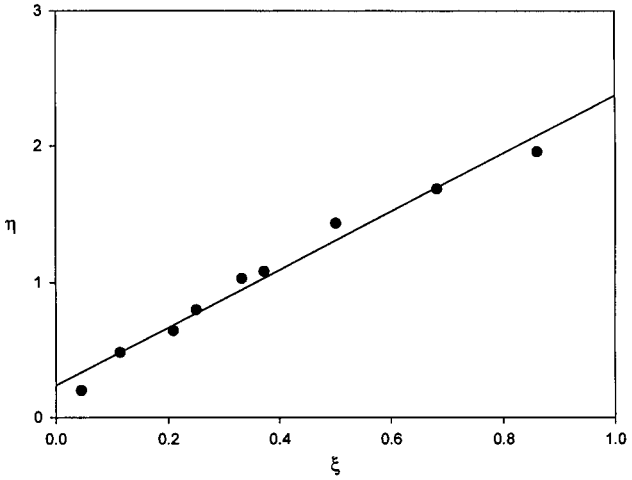

Figure 2. Kelen−Tüdös plot for 4-methyl-1-pentene/ethylene copolymerization with **I**/MAO catalyst.

Table 5. Ethylene/4-Methyl-1-pentene Copolymerization Reactivity Ratios for CpA and Zirconocene Catalysts

catalyst	r_1	r_2	$r_1 r_2$
[Me_2Si(2,3-Me_2−Benz[*e*]Ind)-(N^tBu)]$TiCl_2$ (**I**)	2.14 ± 0.2	0.010 ± 0.002	0.021
[Me_2Si(2-Me−Benz[*e*]Ind)-(N^tBu)]$TiCl_2$ (**II**)	2.26 ± 0.3	0.012 ± 0.003	0.027
[Me_2Si(Benz[*e*]Ind)(N^tBu)]-$TiCl_2$ (**III**)	2.19 ± 0.2	0.010 ± 0.002	0.022
[Me_2Si(Me4Cp)(N^tBu)]$TiCl_2$ (**IV**)	3.81 ± 0.3	0.085 ± 0.004	0.324
[Me_2Si(Ind)(N^tBu)]$TiCl_2$ (**V**)	3.96 ± 0.2	0.087 ± 0.002	0.345
[Me_2Si(Flu)(N^tBu)]$TiCl_2$ (**VI**)	1.19 ± 0.2	0.014 ± 0.002	0.017
[Me_2Si(Flu)(N^tBu)]$ZrCl_2$ (**VII**)	4.56 ± 0.4	0.024 ± 0.005	0.110
rac-Me_2Si(Ind)$_2ZrCl_2$ (**IX**)	28.8 ± 0.8	0.042 ± 0.008	1.210
rac-Me_2Si(Benz[*e*]Ind)$_2ZrCl_2$ (**XI**)	12.7 ± 0.5	0.095 ± 0.02	1.207
rac-Me_2Si(2-Me−Benz[*e*]Ind)$_2$-$ZrCl_2$ (**XII**)	10.8 ± 0.4	0.117 ± 0.03	1.264

the ^{13}C NMR investigation. In contrast, catalysts **IV** and **V,** showing much higher r_2 values (10 times higher) than the catalysts **I**, **II**, **III**, and **VI**, probably encourage 4-methyl-1-pentene homopropagation, and the 4-methyl-1-pentene is slightly clustered to form very short sequence, as confirmed by ^{13}C NMR and DSC analysis. The r_1 and r_2 values for **VI** (r_1 = 1.19; r_2 = 0.014) and **VII** (r_1 = 4.56; r_2 = 0.024) also reflect the metal effect on the 4-methyl-1-pentene/ethylene reactivity ratios.

The product of the reactivity ratios (r_1r_2) for the CpA-catalyzed 4-methyl-1-pentene/ethylene system is much less than 1, indicating a tendency toward alternation, as shown in ^{13}C NMR spectra. This tendency toward alternation is reflected by the observation that, even at very high feed ratios of 4-methyl-1-pentene to ethylene, it is difficult for catalysts **I**, **II**, **III**, and **VI** to incorporate more than 50 mol % of 4-methyl-1-pentene in the copolymers. For example, at the 4-methyl-1-pentene/ethylene mole ratio of 19, the catalyst **I** gives at most 46.4 mol % of 4-methyl-1-pentene in a copolymer (Table 3 and Table 4).

Microstructures of the Poly(ethylene-*co*-4-methyl-1-pentene) Copolymer. The ^{13}C NMR spectra for the three 4-methyl-1-pentene/ethylene copolymers with approximately the same 4-methyl-1-pentene composition (~40.5 mol %), which were prepared with catalysts **I**, **IV**, and **VI**, respectively, are given in Figure 3 as examples. It must be pointed out that the spectra of all copolymers with different 4-methyl-1-pentene incorporation exhibit the same resonances, but with different relative abundance. The chemical shift assignments are

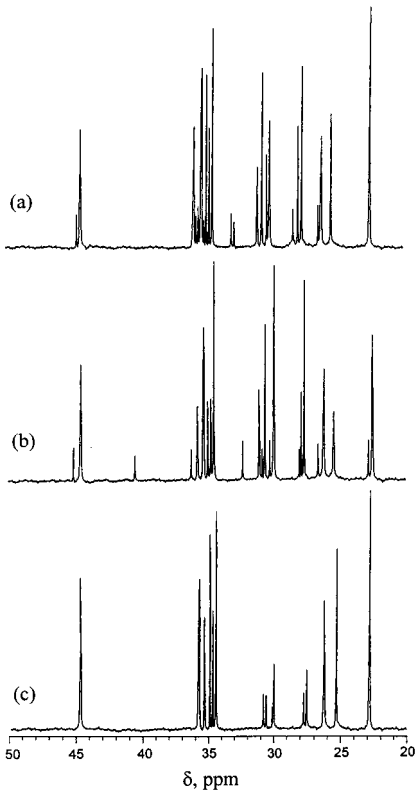

Figure 3. ^{13}C NMR spectra of poly(ethylene-*co*-4-methyl-1-pentene) copolymers prepared by using (a) **I**/MAO catalyst (run 18 in Table 3), (b) **IV**/MAO catalyst (run 4 in Table 2), and (c) **VI**/MAO catalyst (run 6b in Table 2).

listed in Table 6. It is noted that the observed chemical shifts of the carbons are in good agreement with those calculated by the improved Grant and Paul methodology.[25]

As revealed in Figure 3a, the resonance peaks from 22.85 to 44.78 ppm in the aliphatic region of the copolymer produced by **I** (run 18 in Table 3) can be assigned respectively to $S_{\beta\beta}$, $S_{\beta\delta}$, $S_{\delta\delta}$, $S_{\gamma\delta}$, $S_{\gamma\gamma}$, $S_{\alpha\delta}$, $S_{\alpha\gamma}$, and $T_{\delta\delta}$ carbons in the copolymer chain. These carbon resonances in ^{13}C NMR spectrum correspond to an EPE, PEP, EPEP, PEEE, EEEP, EPEE, PEEP, and EEEE sequences of the copolymer (P and E represent the unit of 4-methyl-1-pentene and ethylene, respectively). The ^{13}C NMR spectrum of the **I**-derived P(E-*co*-P) copolymer reveals that formation of PP or PPP sequences is impossible at both very low E/P feed ratios and very high E/P feed ratios. The absence of resonance corresponding to PP or PPP sequences is consistent with very low r_2 values ($r_2 = 0.010 \pm 0.002$) and the copolymerization parameters (r_1r_2 values of 0.021) for the catalyst **I**, indicating a tendency for this catalyst to produce alternating copolymer. In addition, the resonances detected at 26.24, 28.05, 32.81, 32.87, 35.12, 35.26, 35.55, and 44.73 ppm can be assigned to $S_{\alpha\beta}$, $S_{\alpha\delta}$, $S_{\beta\gamma}$, $T_{\gamma\delta}$, and $T_{\gamma\gamma}$, which are due to an ethylene unit bridging head-to-head 4-methyl-1-pentene units (PE**P**E, PEE**P**, PE**P**, and EPE**P** sequences). The extent of head-to-head incorporation of 4-methyl-1-pentene is proportional to its content in the copolymers. The presence of PEE**P**, PE**P**, PE**P**E, and EPE**P** sequences in the copolymer indicates that the insertion of 4-methyl-1-pentene is not completely regioregular. Both secondary and primary insertions of 4-methyl-1-pentene occur at the same time in the 4-methyl-1-pentene/ethylene copolymerization, when the **I**/MAO catalyst is employed. The regioirregular arrangement of 4-methyl-1-pentene units contributes to a significant decrease in the copolymer crystallinity and even led to the disappearance of the crystalline peaks when 4-methyl-1-pentene incorporation in the copolymer is higher than 15 mol % (Table 3). It is apparent that the **I**-derived poly(ethylene-*co*-4-methyl-1-pentene) copolymer has much different microstructures than the heterogeneous Ziegler−Natta catalysts (e.g., $TiCl_4/AlR_3$)[5c,6,7a] and even the previously reported Cp_2M metallocene catalysts.[7a,b]

Table 6. ^{13}C NMR Chemical Shift Assignments for Poly(ethylene-*co*-4-methyl-1-pentene) Copolymer Obtained with CpA Titanium Complexes[a]

carbon type	sequence	chemical shift, ppm: calcd	obsd: cat. **I**	obsd: cat. **IV**	obsd: cat.**VI**
B(1)	EPE	22.88	22.85	22.83	22.88
B(1)	EPPE	22.88		22.94	
$S_{\beta\beta}$	PEP + EPEP	25.23	25.33	25.30	25.25
B(2)	EPE	26.19	26.10	26.12	26.19
B(2)	PE**P**E + PE**P**	26.19	26.24		
B(2)	EPPE	26.45		26.50	
$S_{\beta\delta}$	EPEE	27.62	27.60	27.62	27.58
$S_{\beta\delta}$	PEEP	27.68	27.74	27.76	27.71
$S_{\beta\delta}$	EPPE	27.88		27.91	
$S_{\beta\gamma}$	PEE**P**	28.05	28.12		
$S_{\delta\delta}$	EEEE	29.96	29.98	29.95	29.98
$S_{\delta\delta}$	EPEE	30.07	30.12	30.10	30.08
$S_{\gamma\delta}$	EPEE + PEEE	30.44	30.51	30.50	30.53
$S_{\gamma\delta}$	EPPE	30.64		30.71	
$S_{\gamma\gamma}$	PEEP	30.87	30.95	30.97	30.87
$T_{\beta\delta}$	EPPE	32.30		32.25	
$S_{\alpha\beta}$	EPE**P** + PE**P**E	32.81	32.74		
$S_{\alpha\beta}$	PE**P**	32.87	32.90		
$T_{\delta\delta}$	EPE	34.69	34.59	34.58	34.58
$T_{\delta\delta}$	EPEP	34.75	34.68	34.71	34.70
$T_{\delta\delta}$	PEP	34.81	34.82	34.85	34.83
$T_{\gamma\delta}$	EPE**P**	35.12	35.08		
$S_{\alpha\delta}$	EPE + EPEE	35.20	35.18	35.21	35.28
$S_{\alpha\delta}$	PEE**P** + PE**P**E	35.26	35.30		
$T_{\gamma\gamma}$	PE**P**	35.55	35.61		
$S_{\alpha\gamma}$	PEP + EPEP	35.63	35.70	35.68	35.69
$S_{\alpha\gamma}$	EPPE	36.06		36.12	
$S_{\alpha\alpha}$	EPPE	40.39		40.45	
B(3)	EPE	44.67	44.63	44.65	44.68
B(3)	EPE**P**	44.73	44.78		
B(3)	EPPE	45.10		45.12	

[a] P represents a unit of 4-methyl-1-pentene; the branch carbons are denoted B(*n*) and the number (*n*) in parentheses indicates the position relative to the methyl group in the branch chain; the inverted 4-methyl-1-pentene repeat unit in the copolymer is denoted **P**.

The ^{13}C NMR spectra and the chemical shift assignments also clearly illustrate the different microstructures among the copolymers prepared with **I**, **IV,** and **VI** catalysts, reflecting the influence of the ligand structure of CpA catalysts on the comonomer regioselective insertion (Figure 3b,c). In contrast with catalyst **I**, catalyst **IV** favors the formation of what appear to be consecutive 4-methyl-1-pentene sequence (Figure 3b), which appear as a small resonance peak at 22.94, 26.50, 27.91, 30.71, 32.25, 36.12, 40.45, and 45.12 ppm. These chemical shifts can be assigned to $S_{\beta\delta}$, $S_{\gamma\delta}$, $S_{\alpha\gamma}$, $S_{\alpha\alpha}$, and $T_{\beta\delta}$ carbons in the copolymer containing the EPPE sequence. The observance of resonance corresponding to EPPE sequence is related to higher r_2 values ($r_2 = 0.085$) for the catalyst **IV**. The analysis of the experimental triad distribution of copolymers and the copolymerization parameters (r_1r_2 values of 0.324) indicate a tendency to produce random copolymers. DSC shows that the copolymer containing the EPPE sequence has no melting point (T_m) and crystallinity. More interestingly, the resonance from $S_{\alpha\beta}$, $S_{\alpha\delta}$, $S_{\beta\gamma}$, $T_{\gamma\delta}$, and $T_{\gamma\gamma}$ carbons in the copolymer can no longer be detected in

the **IV**-catalyzed system, suggesting that 4-methyl-1-pentene insertion in the **IV**-catalyzed 4-methyl-1-pentene/ethylene copolymerization proceeds in a regioselective (regioregular) manner.

As shown in Figure 3c, the microstructures of the catalyst **VI**-derived poly(P-*co*-E) copolymers are quite different from those of the copolymers prepared with complex **I** and **IV**. The resonance peaks at 22.94, 26.50, 27.91, 30.71, 32.25, 36.12, 40.45, and 45.12 ppm are no longer detected, indicating that the 4-methyl-1-pentene units in the copolymer are not clustered to form EPPE sequence. At the same time, the resonances at 26.24, 28.12, 32.74, 32.90, 35.08, 35.30, 35.61, and 44.78 ppm disappear, suggesting that the insertion of 4-methyl-1-pentene in the presence of complex **VI** is regioselective. It is notable that, for the **VI**-derived P(E-*co*-P) copolymers, the resonances at 27.58, 27.71, 29.98, 30.08, 30.53, 30.87, and 35.28 ppm of the copolymer are significantly reduced. These resonances can be assigned respectively to $S_{\beta\delta}$, $S_{\gamma\delta}$, $S_{\gamma\gamma}$, $S_{\delta\delta}$, and $S_{\alpha\delta}$ carbons in the copolymer with EPEE, PEEP, EPEE, EEEE, PEEE, and EEEP sequences. In contrast, the resonance peaks at 25.23, 34.58, 34.70, 34.83, and 35.69 ppm assigned to $S_{\beta\beta}$, $S_{\alpha\gamma}$, and $T_{\delta\delta}$ carbons in the copolymer with PEP, EPE, and EPEP sequences increase. These findings suggest that the fluorenyl-based complex **VI** exhibits a pronounced tendency to form alternating distributions of monomers in the polymer chain, which is in a good agreement with the copolymerization parameters ($r_1 = 1.19 \pm 0.2$; $r_2 = 0.014 \pm 0.002$; $r_1 r_2 = 0.017$). Similar behavior of **VI**'s derivative was observed in the ethylene/styrene copolymerization.[11] Further studies are underway to clarify the factors leading to alternating structures formed by this type of catalyst.

Conclusion

These studies show that CpA catalysts, due to their open and accessible active site, can effectively insert 4-methyl-1-pentene into a polyethylene chain in the 4-methyl-1-pentene/ethylene copolymerization. CpA catalysts also provide a higher activity and polymer molecular weight than Cp_2M zirconocenes. However, 4-methyl-1-pentene homopolymerization seems to be lower for CpA complexes than for Cp_2M complexes. Of all the CpA catalysts, the newly synthesized complex [η^5:η^1-(2,3-Me_2-Benz[*e*]Ind)$SiMe_2N^tBu$]$TiCl_2$ (**I**), activated with MAO, exhibits unique catalytic performance. The influence of ligand pattern and the metal atom in CpA complexes on the polymerization and polymer microstructures are significantly noticeable, as shown in the polymerization results, monomer reactivity ratios, and ^{13}C NMR spectra of the polymers. The analysis of ^{13}C NMR spectra illustrates that the regioselectivity of monomer insertion in the 4-methyl-1-pentene homopolymerization is different from that in its copolymerization.

Acknowledgment. The authors thank the National Scientific Foundation of China and Guangdong Province for Young Researchers for the financial support.

References and Notes

(1) (a) Shapiro, P. J.; Bunel, E.; Schaefer, W. P.; Bercaw, J. E. *Organometallics* **1990**, *9*, 867. (b) Stevens, J. C.; Timmers, F. J.; Wilson, D. R.; Schmidt, G. F.; Nickias, P. N.; Rosen, R. K.; Knight, G. W.; Lai, S. Eur. Patent Appl. EP 416 815-A2, 1991 (Dow Chemical Co.). (c) Canich, J. M. Eur. Patent Appl. EP 420 436-A1, 1991 (Exxon Chemical Co.). (d) Chen, Y.-X.; Stern, C. L.; Yang, S.; Marks, T. J. *J. Am. Chem. Soc.* **1996**, *118*, 12451. (e) Kaminsky, W.; Arndt, M. *Adv. Polym. Sci.* **1997**, *127*, 144.

(2) (a) Stevens, J. C. In *Studies in Surface Science and Catalysis;* Hightower, J. W., Delglass, W. N., Iglesia, E., Bell, A. T., Eds.; Elsevier: Amsterdam, 1996; Vol. 101, pp 11−20 and references therein. (b) Chen, Y.-X.; Marks, T. J. *Organometallics* **1997**, *16*, 3649. (c) McKnight, A. L.; Masood, M. A.; Waymouth, R. M.; Straus, D. A. *Organometallics* **1997**, *16*, 2879.

(3) McKnight, A. L.; Waymouth, R. M. *Macromolecules* **1999**, *32*, 2816.

(4) (a) Xu, G.; Sun, Z. Chinese Patent CN 1 192 445, 1998 (Zhongshan University); Chem. Abst. 132: p208279z. (b) Xu, G.; Sun, Z. Chinese Patent CN 1 229 798, 1998 (Zhongshan University); Chem. Abst. 133: p151085x. (c) Xu, G.; Ruckenstein, E. *Macromolecules* **1998**, *31*, 4724.

(5) (a) Tait, P. J. T.; Berry, I. G. In *Comprehensive Polymer Science*; Eastmont, G. C., Ledwith, A. Russo, S., Sigwalt, P., Eds.; Pergamon Press: Oxford, UK, 1989; Vol. 4, p 575. (b) Ver Strate, G. *Encycl. Polym. Sci. Eng.* **1986**, *6*, 522. (c) Boor, J., Jr. *Ziegler−Natta Catalysts and Polymerization*; Academic Press: New York, 1979.

(6) Kimura, K.; Yuasa, S.; Maru, Y. *Polymer* **1984**, *25*, 441.

(7) (a) Burfield, D. R.; Kashiwa, N. *Macromol. Chem.* **1985**, *186*, 2657. (b) Marathe, S.; Mohandas, T. P.; Sivaram, S. *Macromolecules* **1995**, *28*, 7318.

(8) Xu, G.; Lin, S. *Macromolecules* **1997**, *30*, 685.

(9) Foster, P.; Chien, J. C. W.; Rausch, M. D. *Organometallics* **1996**, *15*, 2404.

(10) (a) Nickias, P. N.; Mcadon, M. H.; Patton, J. T.; Friedrichsen, B. P.; Soto, J.; Stevens, J. C.; Vanderlende, D. D. PCT Int. Appl. 97-15583, 1997. (b) Amor, F.; Okuda, J. *J. Organomet. Chem.* **1996**, *520*, 245.

(11) Xu, G. *Macromolecules* **1998**, *31*, 2395.

(12) Okuda, J.; Schattenmann, F. J.; Wocadlo, S.; Massa, W. *Organometallics* **1995**, *14*, 789.

(13) Herrmann, W. A.; Rohrmann, J.; Herdtweck, E.; Spaleck, W.; Winter, A. *Angew. Chem., Int. Ed. Engl.* **1989**, *28*, 1511.

(14) Spaleck, W.; Kuber, F.; Winter, A.; Paulus, E. F. *Organometallics* **1994**, *13*, 954.

(15) Stehling, U.; Diebold, J.; Kirsten, R.; Roll, W.; Brintzinger, H. H.; Jungling, S.; Mulhaupt, R.; Langhauser, F. *Organometallics* **1994**, *13*, 964.

(16) (a) Ethylene Concentration Determination. Ethylene concentrations in toluene can be calculated according to the Henry−Gesetz expression:[16b] $[E] = P_E H_0 \exp(\Delta H_L/RT)$, where [E] is the ethylene concentration (mol/L), P_E is the ethylene pressure in reactor (bar), H_0 is the Henry coefficient (H_0 = 0.001 75 mol/(L bar)), ΔH_L is the enthalpy of solvation for ethylene (ΔH_L = 10 742 W s/mol), R is the universal gas constant, and T is the solution temperature (K). The experimental ethylene concentration is significantly contingent upon the residual nitrogen or argon in solution, the saturation of ethylene in solution, and the accurate pressure change recorded in polymerization system. For our experiments, the differences between observed values with solubility measurements and calculated values are only ±5%. (b) Krauss, V. W.; Gestrich, W. *CHEMTECH* **1997**, *6*, 513.

(17) Mark, H. F.; Bikales, N. M.; Overberger, C. G.; Menges, G. *Encyclopedia of Polymer Science and Engineering*, 2nd ed.; Wiley: New York, 1986; Vol. 4, p 487.

(18) (a) Herrmann, W. A.; Morawietz, M. J. A. *J. Organomet. Chem.* **1994**, *482*, 169. (b) Carpenetti, D. W.; Kloppenburg, L.; Kupec, J. T.; Petersen, J. L. *Organometallics* **1996**, *15*, 1572.

(19) Ruchatz, D.; Fink, G. *Macromolecules* **1998**, *31*, 4684.

(20) Xu, G.; Cheng, D. *Macromolecules* **2000**, *33*, 2825.

(21) Brintzinger, H. H.; Fischer, D.; Mulhaupt, R.; Rieger, B.; Waymouth, R. M. *Angew. Chem., Int. Ed. Engl.* **1995**, *34*, 1143.

(22) Woo, T. K.; Fan, L.; Ziegler, T. *Organometallics* **1994**, *13*, 2252.

(23) The copolymerization parameters were calculated using the Kelen−Tüdös equation:[24] $\eta = r_1\xi - r_2/\alpha(1 - \xi)$; $\eta = G/\alpha + F$ and $\xi = F/\alpha + F$, where x = [ethylene]/[comonomer] in feed and $y = d$[ethylene]/d[comonomer] mole ratio in polymer, $G = x(y - 1)/y$, $F = x^2/y$, $\alpha = (F_m F_M)^{1/2}$, and F_m and F_M are the lowest and highest values of F.

(24) Kelen, T.; Tüdös, F. *React. Kinet. Catal. Lett.* **1974**, *1*, 487.

(25) Randall, J. C. *J. Polym. Sci., Polym. Phys. Ed.* **1975**, *13*, 901.

MA001701J